Monotonic undrained response of early age cemented paste backfill-sand blends

Abdullah Galaa, Murray Grabinsky & Will Bawden
Department of Civil Engineering – University of Toronto, Toronto, Ontario, Canada

2011 Pan-Am CGS Geotechnical Conference

ABSTRACT
The use of cemented paste backfill (CPB) has attracted wide attention in the mining industry world-wide for the past two decades. Liquefaction susceptibility of early age CPB has been a rising concern due to potential risk to mine safety economics. The composition and properties of CPB are mine-specific and may vary within the same mine. Pastefill designers at some mines add sand to the paste mix to improve its pipe-flow characteristics and achieve higher strength. Adding sand to CPB may raise more concerns of its liquefaction susceptibility. In this paper, the effect of adding sand to paste and binder to the paste-sand mixture on liquefaction susceptibility will be addressed. The results of the monotonic undrained triaxial tests on specimens composed of uncemented mine tailings (MT), uncemented MT-Sand mixtures, and CPB-Sand mixtures show that MT as well as the cemented and uncemented mixtures exhibit initial contraction to a certain point where the behaviour changes to dilative. Although adding sand to MT decreases the compressibility and the void ratio of the mix, the undrained behaviour does not show significant changes. The mixture containing the higher sand content exhibits less dilation than the MT samples. As well, mixtures with the higher binder content exhibit less dilation than their uncemented counterparts. State lines obtained from compression and extension tests showed significant anisotropy that increased with the addition of sand and binder. The effect of the axial strain rate on the undrained response was more pronounced for the MT specimens while the strain rate dependence is significantly reduced at a high sand content. In addition, at lower strain rates, the stability of the mixture is enhanced by adding sand.

RÉSUMÉ
Pendant les deux décades passées, l'utilisation des remblais cimentés en pâte (RCP) a attiré une grande attention dans l'industrie minière dans le monde entier. La susceptibilité de liquéfaction de premier âge RCP a été une inquiétude importante en raison de ses conséquences défavorables sur la sécurité et l'économie des mines. La composition et les propriétés de RCP sont spécifiques aux mines et peuvent varier dans la même mine. Les créateurs des remblais à quelques mines ajoutent du sable au mélange de colle pour améliorer ses caractéristiques des pipes d'écoulement et accomplir la plus haute force. Le fait d'ajouter du sable à RCP peut lever plus d'inquiétudes de sa susceptibilité de liquéfaction. Dans cet article, l'effet d'ajouter le sable à la colle et le liant à la mixture de sable et de colle sur la susceptibilité de liquéfaction sera abordé. Les résultats des tests triaxiaux de la monotonique non-drainée sur les exemplaires composés des mines non cimentés, résidus miniers (RM), les mixtures non-cimentée de RM-sable et les mixtures de RCP-sable montrent que RM aussi bien que les mixtures cimentées et non-cimentées exposent la contraction initiale à un certain point où le comportement change pour être dilatif. D'ailleurs, ajoutant du sable à RM diminue la compressibilité et le rapport nul du mélange, le comportement non-drainé ne montre pas de changements significatifs. La mixture contenant le plus haut contenu de sable expose moins d'indicateurs de dilatation que les échantillons de RM. Aussi, les mixtures avec le plus haut contenu de liant exposent moins d'indicateurs de dilatation que leurs contreparties non-cimentées. Les lignes d'état obtenues de la compression et des tests d'extension ont montré une anisotropie significative en ajoutant du sable et du liant. L'effet du taux d'effort axial sur la réaction non-drainée était plus éminentes pour les exemplaires RM pendant que la dépendance de taux d'effort est réduite de façon significative à un haut contenu de sable. En plus, aux taux d'effort plus bas, la stabilité de la mixture est améliorée en ajoutant du sable.

1 INTRODUCTION

Rapid delivery of backfill to support underground opening has enticed many mines to adopt paste backfilling methods. As a precaution to prevent liquefaction and to improve the mechanical performance of backfills, a small portion of a cementitious material (binder) is added to the paste to form the cemented paste backfill (CPB). Cementing paste backfills has proven to provide liquefaction resistance. However, at early ages, before the binder undergoes enough hydration to strengthen the paste, liquefaction susceptibility of CPB is still questionable (le Roux 2004). Particle size distribution of tailings, process water and tailings chemistries, binder type and content, environmental conditions, in addition to many other geometrical and process related factors, are extremely variable even within the same mine. The main concern of this study is to assess the risk of liquefaction when CPB is mixed with sand (CPBS), especially when the active hydration process is delayed under the effect of supplementary cementing materials. The following discussion will review the findings of studies conducted to assess the liquefaction potential of silt-sized CPB under monotonic loads, followed by those conducted on silty sands and gap graded mixtures.

1.1 Liquefaction of Cemented Paste Backfills

Since the 1980's, backfill designers have considered cemented backfill materials as liquefaction resistant if a 100 kPa unconfined compressive strength (UCS) is reached. Clough (1989) suggested this guideline based on a study conducted on round, clean sand. Relying on this "rule of thumb" may be misleading as CPB in most mining operations

have significantly different particle size distributions, particle shapes and chemistries, which may result in completely different binder hydration mechanisms and efficiencies (le Roux, 2004). Several studies have been conducted to assess the liquefaction potential of silt-sized CPB, such as Aref (1989), Pierce et al. (1998), Broomfield (2000), and Been (2002). In all these studies, CPB showed dilative behaviour and no significant pore pressure development in consolidated-undrained (CU) monotonic compression triaxial tests and thereby liquefaction is precluded. However, the earliest curing age among these studies was 2 days in Broomfield (2000).

Rapid rise rates in narrow stopes and the desire to continuously pour, when feasible, have posed more risks of liquefaction at earlier ages than those in the aforementioned studies. Cases where liquefaction potential of CPB is investigated at very early age are very limited. Only le Roux (2004) and Saebimoghaddam (2010) investigated the liquefaction resistance of CPB at ages as early as three hours. The cemented silt-sized gold tailings tested by le Roux (2004) under monotonic compression loading showed that despite the contractive behaviour it exhibited, generated pore water pressures (PWP) were small and the specimens are not susceptible to liquefaction. le Roux (2004) attributed this behaviour to the intensive fabric of the material. Saebimoghaddam (2010) tested cemented and uncemented silt-sized gold tailings in compression and in extension. In compression, cemented and uncemented tailings exhibited stable behaviour that transform from contractive to dilative as strain progresses. In extension, cemented specimens went through temporary instability (limited liquefaction). Uncemented silt-sized tailings were tested by Crowder (2004) and Al Tarhouni (2008) under monotonic compression. Crowder (2004) observed similar behaviour to Saebimoghaddam (2010) but the dilation phase was significantly milder. However, Al Tarhouni (2008) observed limited and flow liquefaction at substantially lower void ratios. In addition, Fourie and Papageorgiou (2001) reported lab and field evidence of flow liquefaction of tailings containing 40% particles larger than 0.075 mm.

At this point, it is useful to discuss the undrained behaviour of tailings and natural soils composed of mixtures of fine and course grained soils. The following paragraphs will be dedicated to this purpose.

1.2 Liquefaction of Silty Sands, Sandy Silts, and Gap Grade Mixtures

Evidence in the literature of the role of nonplastic fines (NPF) on the liquefaction behaviour of sands are contradictory. Kuerbis et al. (1988) have shown that sand with silt content up to 20% exhibited less contraction than cleaner sands under compression and extension loadings. Also, Pitman (1994) observed higher stability with the increase of fines content (FC). On the other hand, Sladen et al. (1985), Ishihara (1993), Lade and Yamamuro (1997), Yamamuro and Lade (1997 and 1998), Fourie and Papageorgiou (2001), Yamamuro and Covert (2001) have reported an increase in contraction with an increase in FC. More recent, Khalili et al. (2010) reported that although the behaviour of paste rock (a highly gap-graded mixture containing around 18% fines) was still controlled by the skeleton of the coarser particles, a reduction in strength is observed when fines were added. Fourie and Papageorgiou (2001) attributed the contradiction in the effect of NPF to the lack of a common basis for comparison. Some studies based their conclusions on whether the steady state line (SSL) moves up or down, and others, such as Yamamuro and Lade (1997), looked at the effect of NPF on liquefaction susceptibility through the relative density. Thevanayagam (2000) and Thevanayagam et al. (2002) presented a different approach based on the arrangement of particles. These studies suggested defining a threshold FC (FC_{th}) which distinguishes between whether the coarse (intergranular) or the fine (interfine) matrix will be dominating the behaviour of the mixture. Consequently, either the actual or an equivalent void ratio of the dominant matrix leads to assessing the liquefaction susceptibility of the whole mixture. From the above discussion, particle arrangement, which is greatly influenced by the packing density, appears to have a major influence on the liquefaction behaviour of a mixture.

1.3 State lines

States of failure or flow can be defined at the points which form unique state lines for a given material. When the material exhibits constant strength with an increasing strain the steady state (SS) is defined. In dilative materials, showing a strain hardening behaviour, defining the SS is difficult (Fourie and Papageorgiou, 2001). In addition, Yamamuro and Lade (1998) reported that the SSL may not always exist for silty sands. Therefore, other states are defined on the basis of uniqueness for a given material. The following discussion will focus on the states associated with dilative behaviours that do not reach a clear steady state.

The critical stress ratio (CSR) is defined when a dilative material undergoes limited liquefaction. The effective stress ratio at the peak deviator stress in the effective stress path represents the CSR points (Chern, 1985, Kuerbis et al., 1988, Thomas, 1992, Al Tarhouni, 2008). Kramer (1996) referred to a unique line that can be plotted as the locus of CSR points as the flow liquefaction surface (FLS) or the temporary instability line (TIL). The phase transformation state (PTS) is another state defined at the point when contraction terminates and dilative behaviour follows. Phase transformation points (PTP) at different densities fall on the same unique line which is referred to as the phase transformation line (PTL) (Thomas, 1992, Al Tarhouni, 2008). Following the PT state, the ultimate failure state (UFS) is reached at maximum stress obliquity (MSO). The unique line plotted as the locus of the maximum stress obliquity points (MSOP) is defined as the ultimate failure envelope/line (UFL).

In the light of this background, an extensive laboratory triaxial testing program was conducted to investigate the influence of mixing CPB with high proportions of sand on the undrained triaxial response at very early curing ages.

2 MATERIALS TESTED

The basic materials used in this testing program involved silica tailings, glacial sand, and binder. All components are supplied by one of Ontario mines in sealed pails. Figure 1 shows the particle size distributions determined in accordance to ASTM C136-06 and ASTM D422-63. The percentage finer than 20 microns in the tailings are around

40%, which is larger than the minimum of 15% suggested to avoid particle settlement and segregation during paste transport and placement. Atterberg limits were determined in accordance to ASTM D4318-05. The liquid limit (LL) of the tailings is 23%, the plastic limit (PL) is 18%, and the plasticity index (PI) is 5%. Therefore, the existing fines are considered non-plastic or “sand-like” fines according to Boulanger and Idriss (2004) where PI of 7 is suggested as the boundary between “sand-like” and “clay-like” fine grained soils. The specific gravity of the tailings is 2.79. X-Ray Fluorescence Spectroscopy (XRF) was performed to determine the chemical composition of the tailings. The summary of the chemical composition is shown in Table 1. The composition presented indicates that the material is rich in silica while alumina can also be considered as a major component. Minor amounts of iron, magnesium and equivalents of calcium and sulphur were also found in their oxide forms. Such low sulphur content is not considered troublesome to the hardening process of CPB as emphasized in many studies on different types of binder (Benzaazoua et al., 1999, 2002, and 2004). The tailings had previously been stored for a long time on surface and might have been subjected to oxidation and alteration; however, all the tests were done on tailings in its current state as used in the CPB mixture.

The glacial sand used at the mine was obtained from native eskers. Glacial sand is naturally silica rich and has not undergone any mineral processing. Therefore, no chemical composition tests were performed as sand is considered inert towards any chemical reaction taking place during binder hydration. The particle size distribution of sand is shown in Figure 1. The specific gravity of sand is 2.70.

The mine used a pre-blended binder provided by Lafarge and comprised of 90% blast furnace slag (BFS) and 10% Type 10 Portland cement (PC). In the construction industry, BFS can compose up to 70% of the blended cement which is significantly lowers than the proportion of BFS in the binder used in this study. BFS improves the workability of the fresh mix, reduces the water demand due to the presence high glassy content, lower the heat of hydration, and alleviates the deleterious effects of an alkali-silica reaction (Simon, 2005). The chemical composition of the binder obtained via XRF is presented in Table 1. The binder primarily contains calcium and silica with minor amounts of magnesium and alumina. The binder is mixed with tailings and sand at 2.2% and 4.5% of the dry weight of solids. Water is added to reach a water content of 28% to generate a paste with a consistency of wet concrete, and a slump of between 140 and 190 mm.

Specimens tested in this study were composed of uncemented 100% mine tailings (MT), uncemented mixture of 55% MT and 45% sand (MTS45), and an uncemented mixture of 45% MT and 55% sand (MTS55). The particle size distribution curves of the uncemented mixtures are shown in Figure 1. According to USCS, the glacial sand is classified as poorly graded sand with some silt, the mine tailings as sandy silt, and the mixtures as poorly graded (moderately gap-graded) silty sands. MTS45 and MTS55, contain 38% and 29% finer than 20 microns; thus, segregation is not expected. Cemented specimens of the same mixtures were also tested at binder contents of 2.2% and 4.5% and will be denoted as CPBS45/2.2, CPBS55/2.2, CPBS45/4.5, and CPBS55/4.5.

Thottarath (2010) investigated the setting characteristics of the cemented mixtures by measuring the electric conductivity (EC) evolution in both CPBS55/2.2 and CPBS55/4.5. The response of EC has shown that the acceleration phase of binder hydration in CPBS55/2.2 and CPBS55/4.5 initiates at 3200 mins (≈53 hours) and 700 mins (≈12 hours), respectively.

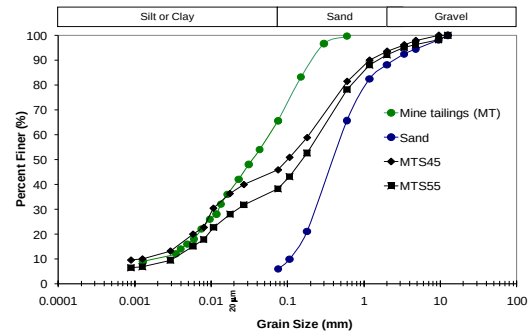

Figure 1 Particle size distribution of the tested materials and mixtures.

3 SAMPLE PREPARATION

Standard preparation methods of triaxial specimens, such as moist placement, dry deposition, and water sedimentation, are not suitable as the components had to be mixed with cement and water in advance of placement. For preparing triaxial CPB specimens of 70 mm diameter, the method suggested by le Roux (2004) and Saebimoghaddam (2010) was followed. Binder, sand, and MT are continuously mixed for 10 minutes at the desired moisture content (28%). Moisture content is then measured prior to casting into the split mould. The mixture is then cast into the mould in three lifts. A glass rod is used to spear each lift around 20 times to remove the large entrained air voids. This “rodding” technique is essentially modified moist tamping (le Roux, 2004). The sample height is measured prior to a one dimensional consolidation process under a 5 kg dead weight (equivalent to about 12.5 kPa) that lasts for one hour. This pressure is equivalent to that exerted by the 0.6 m column of such material with a bulk density of 20 kN/m3 after mixing. Knowing that the rise rate in the stope is 0.25 m/hr, this pressure could be reached after about three hours of filling. Following that, the split mould was removed while the specimens freely stood. The final height and collected water are measured for void ratio calculations. Back saturation followed according to ASTM D4767-04. A minimum B-Value of 0.96 was reached at back pressures ranging between 200 to 250 kPa. The specimen was then hydrostatically consolidated for one hour to reach the desired effective confining pressure (σ'_c). The whole process takes four hours from mixing to loading. Therefore, the binder contribution to liquefaction resistance is expected to be minimal.

To obtain uniform laboratory specimens that result in a representative behaviour of the soil skeleton, oversized particles in the glacial sand were removed prior to mixing with other constituents. This process is known as scalping. The mechanical and hydrological behaviour of the specimen is not affected by the scalping process as long as the removed particles float in the finer matrix (Khalili et al., 2010). For the glacial sand used in this study, the cut-off particle size was 6.3 mm which results in a diameter to maximum grain size

ratio of around 11. The minimum diameter to maximum grain size ratio for a consolidated undrained triaxial test specimen is 6 as suggested by the ASTM D4767-04 while Jamiolkowski et al (2005) expressed 8 as an ideal ratio. In the case presented herein, the removed particles form less than 3% of the mixtures. Therefore, this small fraction is expected to be isolated within the finer soil matrix.

Table 1 Chemical composition of the tailings and binder received from the mine.

Oxide	SiO_2 %	Al_2O_3 %	Fe_2O_3 %	MgO %	CaO %
Tailings	47.1	13.1	6.7	4.8	6.4
Binder	30.5	7.3	0.7	11.1	47.4
Oxide	**Na2O %**	**Ba %**	**SO_3 %**	**K_2O %**	**Others %**
Tailings	1.7	0.1	4.4	2.7	1
Binder	0.4	0.1	1.1	0.5	1.1

4 TESTING PROGRAM

A series of monotonic compression and extension triaxial tests were performed. CU tests were conducted on the uncemented specimens of MT, MTS45 and MTS55 and cemented specimens of CPBS45/2.2, CPBS55/2.2, CPBS45/4.5, and CPBS55/4.5. The experiments were performed at effective confining pressures ranging (σ'_c) ranging from 25 to 400 kPa. The axial loading stage was strain controlled for all experiments at an axial strain rate of 2%/min in compression and of -2%/min in extension. In addition, the response of MT and MTS55 at different strain rates in compression was investigated to validate the use of 2%/min which is higher than the strain rates applied to silty sands and silts.

5 CONSOLIDATION RESPONSE

At the end of the hydrostatic consolidation stage, the response of volumetric strain (ε_v) and axial strain (ε_a) for the triaxial specimens was measured. The gradients of the best-fit lines which represent ($\Delta\varepsilon_v/\Delta\varepsilon_a$) was obtained from ε_v versus ε_a plots. Table 2 shows the values of the gradients which ranged from 3.18 to 3.68 depending on the mixture. Perfect isotropic response should result in gradients of 3.0. Deviations from this value suggest an anisotropic material fabric. From Table 2, it appears that adding sand resulted in a more anisotropic response which increased by increasing the sand content. Adding binder to MT-sand mixtures generally reduced its anisotropy which appears to decrease by increasing the binder content. The gradients of cemented and uncemented mixtures compare well with those presented by Khalili et al. (2010).

Compressibility response of all specimens consolidated under stresses ranging from 25 to 400 kPa was recorded. The calculated compression indices (C_c) were calculated and summarized in

Table 3.

Adding sand or sand and binder drastically changed the value of C_c. When only sand was added to MT, C_c decreased around 70%. When binder is added to the MT-Sand mixture, C_c increased around 100%, thus bringing the compressibility back close to that of MT. Although the compressibility of MTS45 was too close to MTS55, cemented specimens with higher sand content (CPBS55) had lower compressibility than that of the lower sand content (CPBS45) and increasing the binder content has significantly decreased the compressibility in comparison to the lower sand content. The question that should be answered in the fore coming sections is whether such mixtures with different compressibility differently behave under monotonic loading.

Table 2 Gradients of the best-fit lines indicating $\Delta\varepsilon_v/\Delta\varepsilon_a$ values

Specimen	**MT**	**MTS45**	**MTS55**	**CPBS45/2.2**
$\Delta\varepsilon_v/\Delta\varepsilon_a$	3.18	3.48	3.62	3.37
Specimen	**CPBS45/4.5**	**CPBS55/2.2**	**CPBS55/4.5**	
$\Delta\varepsilon_v/\Delta\varepsilon_a$	3.32	3.68	3.55	

Table 3 Compression indices for the tested MT, MTS, and CPBS specimens.

Material	**MT**	**MTS45**	**MTS55**	**CPBS45/2.2**	**CPBS45/4.5**	**CPBS55/2.2**	**CPBS55/4.5**
C_c	0.048	0.016	0.017	0.036	0.035	0.03	0.025

6 UNDRAINED RESPONSE IN TRIAXIAL COMPRESSION

The stress path results in this study will be presented in the s´-t space. The variables normal stress ($s' = (\sigma'_1+\sigma'_3)/2$) and the shear stress ($t = (\sigma'_1-\sigma'_3)/2$) are used. In Mohr stress space, s' and t represent the top point of the Mohr circle representing the stress state at any moment during the test. The state line has an inclination of ϕ' in Mohr stress space while it has an inclination of α' in the s'-t space. The relation between the inclinations of same state line in both Mohr and s´-t stress spaces can be correlated by $\tan \alpha' = \sin \phi'$. The stress states of interest will be at the PTS and the UFS.

6.1 Uncemented mine tailings

This section presents the monotonic test results for five MT specimens at σ'_c ranging from 25 to 400 kPa (Figure 2). Figure 2a shows the undrained stress paths of MT specimens and the void ratios. FC in MT specimens was 70%. All the specimens experienced the same initial contractive behaviour followed by dilative behaviour. The initial tendency to contraction is translated into an increase pore water pressure generation and deviation from the hypothetical drained path. The tendency to contraction terminates when the pore water pressure reaches a maximum value (Δu_{max}) at the PTP, beyond which the specimens tend to dilate and the decrease in the pore water pressure is evidence of the dilation tendency. Dilation of specimens decreases with increasing σ'_c. Figure 2b shows the pore pressure ratio r_u ($\Delta u/\sigma'_c$)

versus strain. A good statistical fit of the PTL is obtained by defining the unique PTP in the *s´-t* space for each specimen. The PTL has an angle of α'_{PTL}= 29.2^o in the *s´-t* space.

All specimens exhibit a strain hardening behaviour where neither flow liquefaction nor temporary liquefaction was observed at all σ'_c. The Shear stress (*t*) increases indefinitely without reaching a plateau and the excess PWP decreases asymptotically indicating that no steady state was reached until the tests were stopped at approximately 20% strain. For such silty material, however, the UFL can be defined at maximum stress obliquity points (MSOP) (i.e. maximum $t/s' = (\sigma'_1-\sigma'_3)/(\sigma'_1+\sigma'_3)$). This state is temporarily reached then the ratio *t/s´* deviates from the horizontal and this deviation decreases by increasing σ'_c. A good statistical fit of UFL to the maximum *t/s´* points in the *s´-t* space has an angle of α'_{UFL}= 31.0^o in the *s´-t* space. A summary for the slopes of the UFL and PTL of all the mixtures is presented in Table 4.

6.2 Uncemented MT-Sand mixtures

Five MTS45 specimens were tested at σ'_c ranging from 25 to 400 kPa. The void ratio ranged from 0.385 to 0.340 and FC was 45.8%. The entire set of specimens exhibited similar behaviour to that of the MT specimens. The angles of the UFL and the PTL in the *s´-t* space are only within the order of two degrees higher than that of MT (see Table 4).

The monotonic test results for three MTS55 specimens and their void ratios at different σ'_c are shown in Figure 3. FC in MTS55 specimens was 38.2%. All MTS55 specimens exhibited similar behaviour to that of MT and MTS45 specimens. Although a MTS55 has a larger percentage of course grained particles, the dilation tendency is significantly less than in the case of MT and MTS45. The angles of the UFL and the PTL are only within the order of one degree less than that of MTS45 (see Table 4). In addition, MTS55 specimens showed more contraction and less dilation than MT and MTS45.

Table 4 Slopes of the UFL, PTL and TIL, in the s´-t space, from compression and extension triaxial testing at 2%/min.

	Compression		Extension		
	α_{UFL}	α_{PT}	α_{UFL}	α_{PT}	α_{TIL}
MT	31.0	29.2	28.0	22.7	13.1
MTS45	32.3	31.3	27.6	22.8	13.2
MTS55	31.6	30.6	26.1	19.3	11.3
CPBS45/2.2	32.3	31.6	23.6	17.3	10.9
CPBS45/4.5	33.7	33.2	24.5	19.9	11.4
CPBS55/2.2	32.8	32.3	24.0	19.5	11.8
CPBS55/4.5	32.8	31.7	24.1	18.4	10.8

6.3 Cemented paste backfills with sand

Specimens of CPBS45/2.2, CPBS55/2.2, CPBS45/4.5, and CPBS55/4.5 were tested and the results of CPBS45/4.5 and CPBS55/4.5 are shown in Figure 4 and Figure 5, respectively. It is worth mentioning that binder content contributes to the FC calculated for each cemented specimen. The behaviour of the cemented specimens is essentially similar behaviour to that of the MT-Sand mixtures. At both sand contents, the rate of dilation is milder than that of their uncemented counterparts. This is more pronounced in the case of 4.5% binder. The angles of the UFL and the PTL in the *s´-t* space are only within the order of 1.5^o higher than that their uncemented counterparts (see Table 4). No particular relationship was observed between the slopes of the state lines and the binder content.

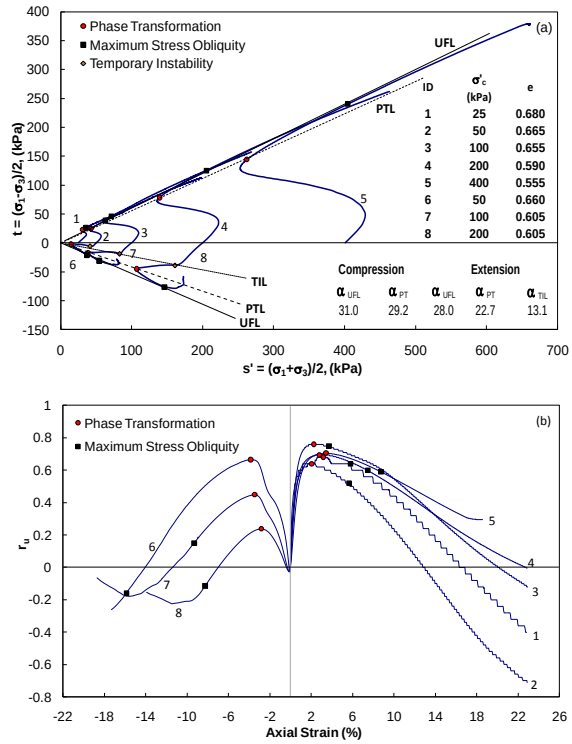

Figure 2 Monotonic response of 100% mine tailings (MT). (a) Stress path and (b) Pore pressure ratio, ru, versus axial strain.

6.4 Effect of strain rate on uncemented specimens

Strain rate values in strain controlled triaxial testing are usually determined to ensure pore water pressure equilibration during the test. In this study, the strain rate (2%/min) under which the specimens were loaded is significantly higher than the common values used for materials of similar hydraulic conductivity. However, the reason behind working at a relatively high strain rate is to minimize the effect of the ongoing hydration process on the response of the cemented blends during the experiment. Uncemented specimens are tested at the same strain rates for the sake of comparison. Knowing that the strain rate influences the behaviour of materials, it was important to investigate the possible variation in behaviour caused by changing the strain rate. MTS55 specimens were chosen to be tested at different strain rates as it is the most commonly used mixture at the mine, while MT specimens were also tested as control specimens to emphasize how adding sand may affect the behaviour at different strain rates. Consistent void ratios are obtained when specimens are hydrostatically consolidated under σ'_c = 200 kPa; therefore, monotonic compression tests are conducted at this stress level.

Four specimens of MTS55 were tested at σ'_c = 200 kPa under axial strain rates of 2%, 1%, 0.1%, and 0.02%/min. The pre-shearing void ratios were 0.320±0.005. All the specimens

exhibited the same behaviour as that of the 2%/min specimen. Although PWP generated at lower strain rates was slightly higher than that at 2%/min, it neither changed the behaviour nor the location of the state lines if plotted for each specimen individually.

Three MT specimens were tested at σ'_c = 200 kPa under axial strain rates of 2%, 0.05%, 0.02%/min. The pre-shearing void ratios were 0.61±0.005. In this case, where no sand is added, the behaviour at lower strain rates is significantly different from that of the 2%/min specimen (see Figure 6). PWPs generated at 0.05% and 0.02%/min are significantly higher than that generated at 2%/min as can be seen in Figure 6b. Although the higher PWP brought MT specimen towards more instability, the specimen did not exhibit explicit limited liquefaction behaviour. In contrast to the rest of the specimens tested in this study, the specimen tested at 0.05%/ min exhibited a strain softening behaviour and the specimen tested at 0.02%/ min exhibited a very mild strain hardening behaviour. Locations of the state lines did not change.

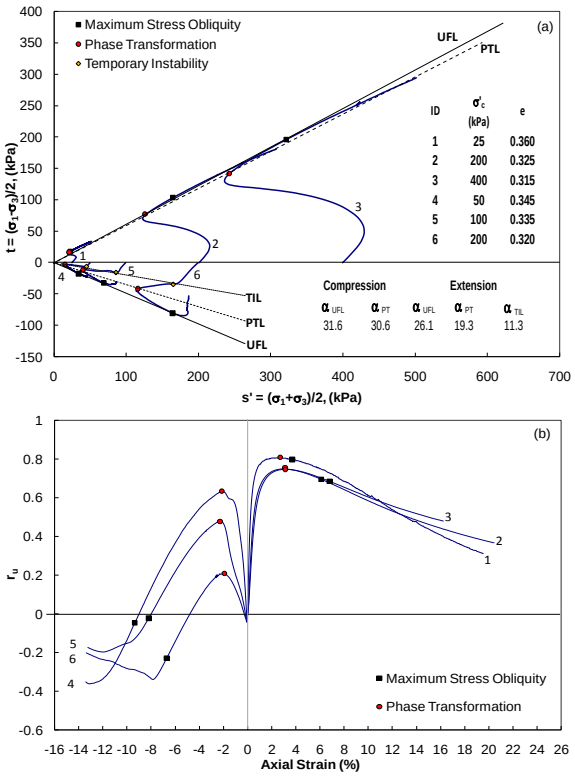

Figure 3 Monotonic response of uncemented MTS55. (a) Stress path and (b) Pore pressure ratio, ru, versus axial strain.

7 UNDRAINED RESPONSE IN TRIAXIAL EXTENSION

MT, MTS, and CPBS specimens were subjected to undrained extension loading at a strain rate of -2%/min. The behaviour of MT, MTS, and CPBS specimens was generally the same. The material starts as contractive and transfers to dilative at a unique point until it reaches UFL. However, and in contrast to compression, all specimens exhibited temporary instability before going through phase transformation. Extension results are shown in Figure 2 to Figure 5. Necking was observed for all samples tested at 100 and 200 kPa. Necking can be defined at the end of the dilation phase in the r_u plots. It was also observed that necking occurred at smaller strains as σ'_c increased.

A good statistical fit of the flow liquefaction or the TIL is obtained by defining a unique temporary instability point (TIP) in the *s´-t* space for each specimen and the angles are summarized in Table 4. Angles of the UFL and PTL for all specimens (MT and mixtures) in extension are lower than those in compression which may be attributed to anisotropy. In the case of MT specimens, the difference between the angles of these state lines in compression and extension is about 3° for the UFL and is about 6.5^o for the PTL, all expressed in the *s´-t* space. By adding sand this difference increases indicating higher anisotropy. The difference is in the order of 5° for the UFL and is about 10° for the PTL for both sand contents. Adding binder to the MT-sand mixtures increased the difference more than for the uncemented counterparts indicating much higher anisotropy in the case of CPBS. The difference is in the order of 9° for the UFL and is about 13° for the PTL for both sand contents. This difference did not show any particular pattern of change by changing the binder content. Genrally, when comparing uncemented MT-sand mixtures to MT, the angles of the UFL and the PTL are only within the order of 2° less than those of MT. Moreover, when comparing cemented MT-sand mixtures (CPBS) to their uncemented counterparts, the angles of the UFL and the PTL are within the order of 3° less.

In contrast to the behaviour in compression, σ'_c had a great influence on PWP generation. For all specimens, the generated PWP significantly decreased by increasing σ'_c indicating higher stability. This agrees with the results presented by Saebimoghaddam (2010). This influence is less pronounced in the cemented specimens.

8 DISCUSSION

For a better understanding of the materials' behaviour, the UFLs obtained from compression and extension tests are plotted in the global void ratio versus the mean effective stress (*e-log p'*) space and shown Figure 7. From these plots, it can be seen that the UFL of each of the cemented mixtures are not affected by the binder content and their position remained almost the same. Compression and extension state lines are plotted on the same scale for the sake of comparison. The positions of the UFLs obtained from extension tests, compared with those obtained from compression tests, are almost identical for all materials except for MT which showed a slight difference between the slopes in the *e-log p'* space. This observation may seem to contradict with the previous observation of unequal slopes of the state lines, in the *s'-t'* space, obtained from compression and extension. Most studies have suggested that this inequality in the *s'-t'* space is a result for the anisotropy of the soil fabric (for example, Vaid and Thomas (1995), Khalili et al. (2010), Saebimoghaddam (2010)). However, Riemer (1997) obtained three different SSL by testing fine sand in triaxial compression, triaxial extension, and simple shear. He attributed the differences to different stress paths followed in the different tests. One reason for having an evidence of

anisotropy from compression and extension results in the *s'-t'* space while not having the same in the *e-log p'* space, in this study, could be due to having pre-shearing void ratios too close to the void ratio at the UFS.

Saebimoghaddam (2010) conducted a similar study, using the same apparatus, on a different mine tailings material that contained only 10% particles larger than 0.075 micron. He observed anisotropy but not to same extent even when compared with MT specimens tested in this study. The higher anisotropy in this study could be attributed to higher coarse grained fraction in all specimens relative to what Saebimoghaddam (2010) tested. Furthermore, significant differences in particle fabrics were observed from the SEM images shown in Figure 8. MT tested in this study has more flakey particles and a substantial particle size gap, as shown in Figure 8a. Whereas, particles of Williams mine tailings tested by Saebimoghaddam (2010) are more rounded and uniform (Figure 8b). The more flakey particles might be the reason for a more anisotropic fabric.

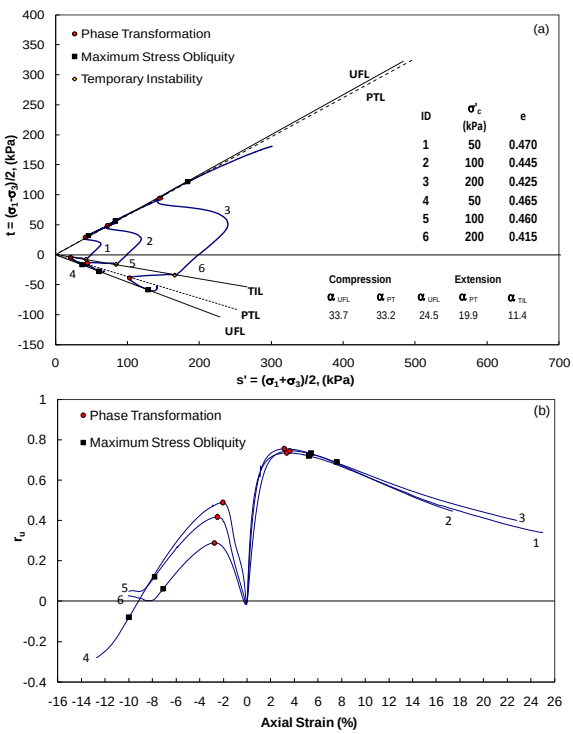

Figure 4 Monotonic response of CPBS45/4.5 cured for 4 hours. (a) Stress path, (b) Pore pressure ratio, ru, versus axial strain.

Another observation that could be made from Figure 7 is that the UFL of CPBS specimens are parallel to that of the MT and not to that of their uncemented counterparts (MTS). Also, the values of C_c for CPBS are closer to that of the MT rather than that of their uncemented counterparts. This could be an indicator that although the increase in FC due adding binder is very small, adding binder to MT-sand mixtures increases the dominance of the finer matrix to the behaviour of the overall mixture. From all the above, it can be asserted that adding binder has positively impacted the behaviour in compression, while negatively impacted the behaviour in extension.

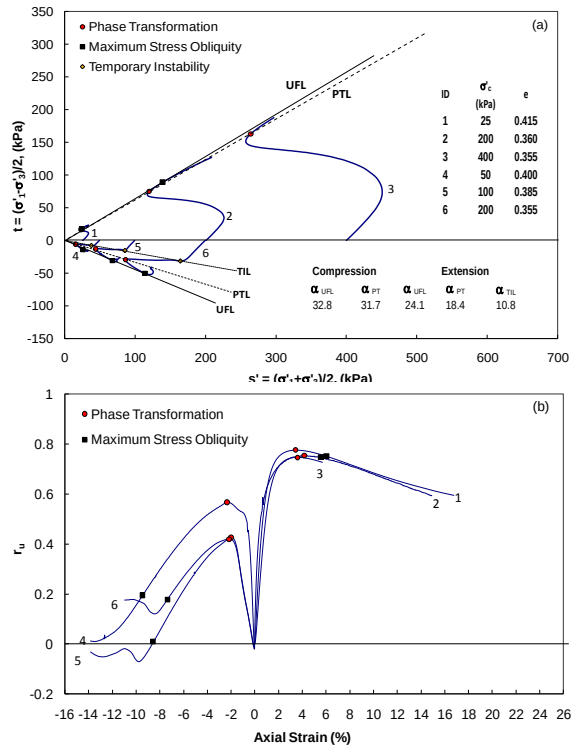

Figure 5 Monotonic response of CPBS55/4.5 cured for 4 hours. (a) Stress path, (b) Pore pressure ratio, ru, versus axial strain.

9 CONCLUSION

An extensive triaxial testing program was performed to investigate the effect of adding sand or sand and binder on the liquefaction potential and mechanical behaviour of mine tailings. Generally, no flow liquefaction was observed for MT, MTS or CPBS (cured at four hours) under monotonic compression loading. All specimens exhibited limited instability under monotonic extension loading and σ'_c had a great influence on PWP generation, in contrast to the compression specimens. The addition of sand to MT reduced the compressibility of the mixture. The slopes of the state lines in the *s'-t'* space increased in compression while decreased in extension. Specimens exhibited higher anisotropy when sand was added to MT by comparing extension and compression state lines.

The addition of binder to MT-sand mixtures increases the compressibility of the mixture to be close to those of MT. The slopes of the state lines in the *s'-t'* space increased in compression while decreased in extension compared to their uncemented counterparts. Cemented specimens exhibited higher anisotropy by comparing extension and compression state lines. Generally, the behaviour did not change by adding binder. However, less dilation was observed especially at the higher sand content.

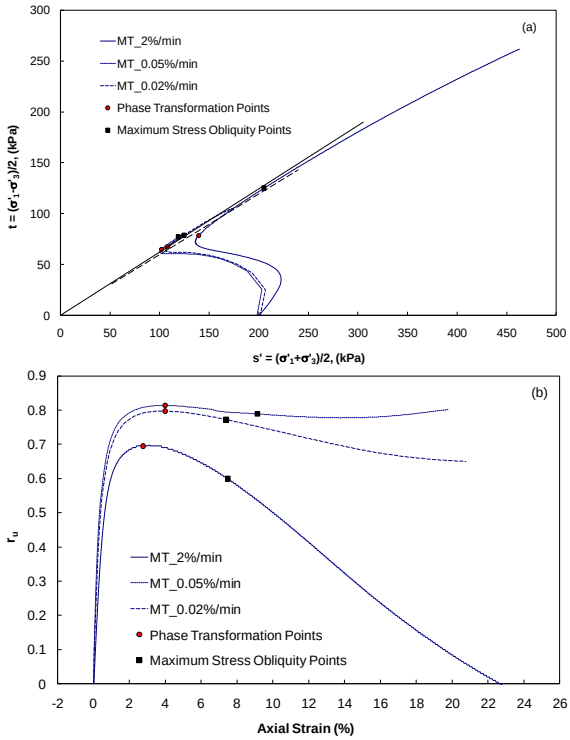

Figure 6 Monotonic response of MT at σ'_c = 200 kPa different strain rates. (a) Stress path, (b) Pore pressure ratio, ru, versus axial strain.

The behaviour of MT dramatically changed at lower strain rates towards a more unstable behaviour. However, no temporary instability was observed. On the other hand, MTS55 exhibited no significant changes by changing the strain rate. Therefore, adding 55% sand eliminated the strain rate dependence observed with MT.

Analyzing the state lines in the *e-lop p'* space showed that anisotropy and stress path effects were not emphasized by plotting extension and compression state lines. Also, state lines in the *e-log p'* and C_c values showed that the behaviour of CPBS is influenced by the finer fraction.

In the field, the rock walls closure can impose a stress path too close to that of the extension tests, under which the material exhibited a weaker response and temporary liquefaction. The preparation method followed in this study is believed to resemble the field placement technique. However, further research is needed to obtain CPB specimens at higher void ratios. This will help in cases of narrow stopes where rise rates are significantly higher.

10 ACKNOWLEDGEMENT

The project is supported financially by Barrick Gold Corporation, Xstrata Copper Canada, Inmet Mining Corporation, and the Natural Sciences and Engineering Research Council Canada (NSERC).

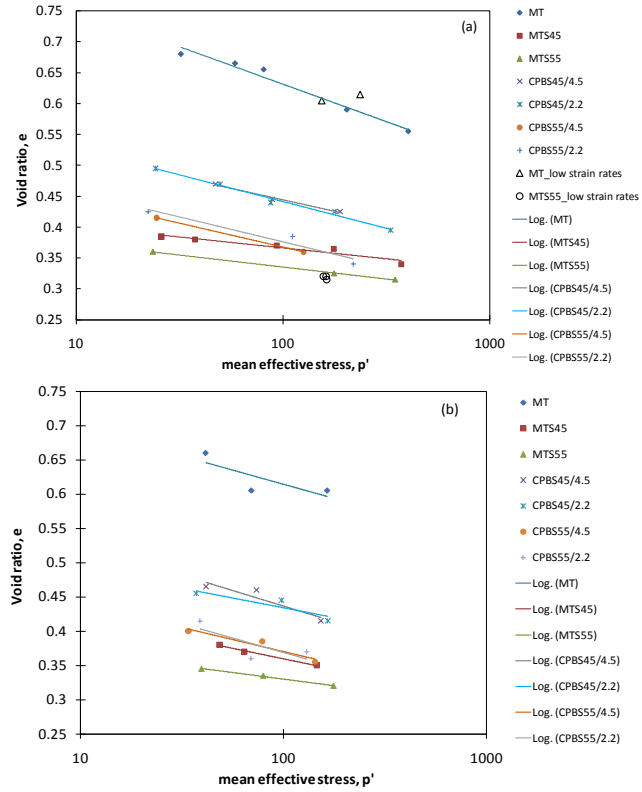

Figure 7 e-lop p' plots showing (a) UFL in compression and (b) UFL in extension.

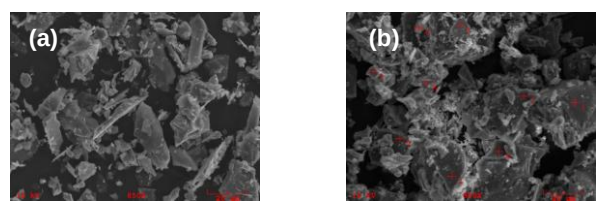

Figure 8 SEM images of (a) MT tested in this study and (b) Williams MT tested by Saebimoghaddam (2010).

11 REFERENCES

Al Tarhouni, M. 2008. *Liquefaction and post-liquefaction behaviour of gold mine tailings under simple shear loading*. M.A.Sc., Carleton University, Canada.

Aref, K. 1989. *A study of the geotechnical characteristics and liquefaction potential of paste backfill*. Ph.D., McGill University, Montreal, Canada.

ASTM C136 2006. Standard test method for sieve analysis of fine and coarse aggregates. *The Annual Book of ASTM Standards*, Sect 4, Vol. 04.02.

ASTM D422–63 2007. Standard test method for particle size analysis of soils. *The Annual Book of ASTM Standards*, Sect 4, Vol. 04-08.

ASTM D4318–05 2007. Standard test methods for liquid limit, plastic limit, and plasticity index of soils. *The Annual Book of ASTM Standards*. Sect 4, Vol. 04-08.

ASTM D4767 2004. Standard test method for consolidated undrained triaxial compression test for cohesive soils. *The Annual Book of ASTM Standards*, Sect 4, Vol. 04-08.

Been, K. 2002. Liquefaction potential of paste fill at neves corvo mine, portugal, *Transactions of the Institution of Mining and Metallurgy*. Section: A Mining industry, 111(1): 47.

Benzaazoua, M., Fall, M., and Belem, T. 2004. A contribution to understanding the hardening process of cemented pastefill, Minerals Engineering, 17(2): 141-152.

Benzaazoua, M., Belem, T., and Bussière, B. 2002. Chemical factors that influence the performance of mine sulphidic paste backfill, *Cement and Concrete Research*, 32(7): 1133-1144.

Benzaazoua, M., Ouellet, J., Servant, S., Newman, P., and Verburg, R. 1999. Cementitious backfill with high sulfur content physical, chemical, and mineralogical characterization, *Cement and Concrete Research*, 29(5): 719-725.

Boulanger, R.W. and Idriss, I.M., 2004. *Evaluating the potential for liquefaction or cyclic failure of silts and clays*. Report No. UCD/CGM-04/01, Center for Geotechnical Modeling, University of California, Davis, CA, 130 p.

Broomfield, D. 2000. *Liquefaction potential of paste backfill*. M.Sc., Queen's University, Canada. .

Chern, J. 1985. *Undrained response of saturated sands with emphasis on liquefaction and cyclic mobility*. PhD, The University of British Columbia, Canada.

Clough,G.W. 1989. Influence of cementation on liquefaction of sands. *Journal of Geotechnical Engineering*, 115: 1102-17.

Crowder, J.J. 2004. *Deposition, consolidation, and strength of a non-plastic tailings paste for surface disposal*. Ph.D., University of Toronto, Toronto, Canada.

Fourie, A.B. and Papageorgiou, G. 2001. Defining an appropriate steady state line for merriespruit gold tailings. *Canadian Geotechnical Journal*, 38(4): 695-636.

Ishihara, K. 1993. Liquefaction and flow failure during earthquakes, *Geotechnique*, 43(3): 351-415.

Jamiolkowski, M., Kongsukprasert, L., and Lo Presti, D. 2005. Characterization of gravelly geomaterials. *In Proceedings of The Fifth International Geotechnical Conference*, Cairo, Egypt, 12 January 2005. pp. 1–27.

Khalili, A., Wijewickreme*, D., and Wilson, G. 2010. Mechanical response of highly gap-graded mixtures of waste rock and tailings. part I: Monotonic shear response, *Canadian Geotechnical Journal*, 47(5): 552-565.

Kramer, S.L. 1996. *Geotechnical earthquake engineering*. Prentice Hall, Upper Saddle River, N.J.

Kuerbis, R., Negussey, D., and Vaid, Y.P. 1988. Effect of gradation and fines content on the undrained response of sand. *In Hydraulic Fill Structures*, pp. 330-345.

Lade, P.V. and Yamamuro, J.A. 1997. Effects of nonplastic fines on static liquefaction of sands, *Canadian Geotechnical Journal*, 34(6): 918-928.

le Roux, K. 2004. *In situ properties and liquefaction potential of cemented paste backfill.* Ph.D., University of Toronto, Toronto, Canada.

Pierce, M., Bawden, W.F., and Paynter, J.T.Laboratory testing and stability analysis of paste backfill at the golden giant mine. *In Minefill '98: Proceedings of the 6th International Symposium on Mining with Backfill*, Brisbane, pp. 159–165.

Pitman, T.D. 1994. Influence of fines on the collapse of loose sands, *Canadian Geotechnical Journal*, 31(5): 728-739.

Riemer, M. 1997. Factors affecting apparent position of steady-state line. *Journal of Geotechnical and Geoenvironmental Engineering*, 123: 281-8.

Saebimoghaddam, A. 2010. *Liquefaction of early age cemented paste backfill*. PhD, University of Toronto, Toronto, Canada.

Simon, D. 2005. *Microscale analysis of cemented paste backfill*. Ph.D., University of Toronto, Toronto, Canada.

Sladen, J.A., D'Hollander, R.D., Krahn, J., and Mitchell, D.E. 1985. Back analysis of the nerlerk berm liquefaction slides, *Canadian geotechnical journal*, 22(4): 579-588.

Thevanayagam, S. 2000. Intergranular state variables and stress-strain behaviour of silty sands, *Géotechnique*, 50(1): 1-23.

Thevanayagam, S., Shenthan, T., Mohan, S., and Liang, J. 2002. Undrained fragility of clean sands, silty sands, and sandy silts, *Journal of Geotechnical and Geoenvironmental Engineering*, 128(10): 849-859.

Thomas, J. 1992. *Static, cyclic and post liquefaction undrained behaviour of fraser river sand*. MASc, The University of British Columbia, Canada.

Thottarath, S. 2010. *Electromagnetic Characterization of Cemented Paste Backfill in the Field and Laboratory*. MASc, The University of Toronto, Canada.

Vaid, Y.P. and Thomas, J. 1995. Liquefaction and postliquefaction behavior of sand, *International Journal of Rock Mechanics and Mining Sciences & Geomechanics Abstracts*, 32(8, pp. 379A-379A): December.

Yamamuro, J.A. and Lade, P.V. 1997. Static liquefaction of very loose sands, *Canadian geotechnical journal*, 34(6): 905-917.

Yamamuro, J.A. and Covert, K.M. 2001. Monotonic and cyclic liquefaction of very loose sands with high silt content, *Journal of Geotechnical and Geoenvironmental Engineering*, 127(4): 314-324.

Yamamuro, J.A. and Lade, P.V. 1998. Steady-state concepts and static liquefaction of silty sands, *Journal of Geotechnical and Geoenvironmental Engineering*, 124(9): 868-877.